Intercomparison Study of the Land Surface Process Model and the Common Land Model for a Prairie Wetland in Florida

B. WHITFIELD

Department of Civil and Coastal Engineering, University of Florida, Gainesville, Florida

J. M. JACOBS

Department of Civil Engineering, University of New Hampshire, Durham, New Hampshire

J. JUDGE

Department of Agricultural and Biological Engineering, Center for Remote Sensing, University of Florida, Gainesville, Florida

(Manuscript received 15 August 2005, in final form 21 March 2006)

ABSTRACT

Common Land Model (CLM) and Land Surface Process (LSP) model simulations are compared to measured values for a 13-day dry-down period with a rapidly decreasing near-surface water table for a marsh wetland community in Florida. LSP was able to provide reasonable estimates without any modifications to the model physics. To obtain reasonable simulations using CLM, the baseline TOPMODEL baseflow generation and the bottom drainage mechanisms were not employed and the lower layers were allowed to remain saturated. In addition, several of CLM's default wetland vegetation parameters were replaced with grassland parameters. Even after these modifications, CLM underestimated soil water storage. However, both model-simulated soil temperatures showed very good agreement as compared to measured temperatures, capturing both the soil warming during the study period and the diurnal fluctuations. Modeled surface energy fluxes also agreed well with measured values. LSP's inability to consistently capture latent heat fluxes appears to be linked to its canopy resistance scaling functions. Other minor issues were that CLM's rooting depth greatly exceeded observed depths and that CLM did not move water in the vadose zone from lower to upper layers during the nighttime as observed in the measurements. Overall, these results suggest that LSP can be applied to characterize a marsh dry down, but that minor modifications could greatly improve results. CLM demonstrated considerable potential, but requires some changes to model physics and default parameters prior to application to wetlands at a subgrid scale.

1. Introduction

Wetlands, covering between 4% and 6% of the earth's land surface, are distinguished by near-surface water tables with unique plants and soils (Mitsch and Gosselink 2000). North America has approximately one-third of the world's wetlands with an area of about 240 million ha, including 107 million ha in the United States (Hall et al. 1994). Swamps and marshes include 90% of all inland wetland communities in the lower 48 states of the United States. Both swamps and marshes have fluctuating water tables and are defined by their hydroperiods that routinely include soil inundation and dewatering. The defining characteristics of swamps and marshes are their differences in vegetation type. Swamps have trees and shrubs while marshes are treeless with grasses, sedges, and aquatic plants.

Because wetlands have saturated soils and high water tables, evapotranspiration is typically at or near potential and water and energy exchange is relatively high. Wetlands also have a distinct role in methane emissions and global carbon storage and cycling. Plant decomposition, plant carbon fixation, and methane production and function are highly dependent on water table and soil temperature (Zhang et al. 2002).

Soil–vegetation–atmosphere transfer models (SVAT) offer significant capabilities to predict wetland water

Corresponding author address: Jennifer M. Jacobs, Department of Civil Engineering, 240 Gregg Hall, 35 Colovos Road, University of New Hampshire, Durham, NH 03824-3534.
E-mail: Jennifer.Jacobs@unh.edu

dynamics and soil temperature and moisture states. By constraining both the water and the energy balance, SVATs are routinely used to model land surface fluxes, root zone soil water states, and temperature signals for hydrological, climate, and biogeochemistry studies. The overall success of SVATs has been demonstrated through model intercomparison studies such as the Project for Intercomparison of Land Surface Parameterization Schemes (PILPS; Henderson-Sellers et al. 1995), the Global Soil Wetness Project (GSWP; Dirmeyer et al. 1999), and various site-specific studies. Intercomparison studies identify SVAT strengths and characterize differences among models. For example, the PILPS phase 2's four site intercomparison found better agreement between modeled and measured latent heat fluxes than either sensible heat or ground heat fluxes for simulations without snow cover (Shao and Henderson-Sellers 1996; Chen et al. 1997; Liang et al. 1998). Single model validation studies have detailed model strengths and weaknesses across landscapes and climatic conditions (Nijssen et al. 1997; Mohr et al. 2000; van der Keur et al. 2001). Such studies have considered midlatitude grasslands and croplands (Liou et al. 1999; Mohr et al. 2000), boreal forests and arctic tundra (Nijssen et al. 1997; Kim 1999; Slater et al. 2001), and tropical forests (Pitman et al. 1999).

Although SVAT calibration/validation research includes several regions and climate types, few SVAT validation studies have considered wetlands. Comer et al. (2000) found that the wetland processes in the Canadian Land Surface Scheme (CLASS) were able to characterize energy fluxes in fens and marshes, but was unsuccessful for bogs due to their nonvascular vegetation. Lafleur (1990), Souch et al. (1998), and Jacobs et al. (2002a) found that energy partitioning in marsh ecosystems is a function of water table or wetland soil moisture. However, it is unknown how SVATs behave during wetting and drying down of wetlands. At Comer et al.'s (2000) marsh site, CLASS consistently underestimated all latent heat fluxes whose magnitude exceeded 200 W m^{-2}. Because the bias appeared to decrease immediately following the precipitation event, there were potential issues with dewatering and characterization of the soil water state.

The purpose of this paper is to validate the performance of two SVAT models during a 13-day dry-down period with a rapidly decreasing near-surface water table for a marsh in the southeastern United States. The limited study period allows for a focused examination of model results under rapidly evolving conditions without precipitation. The two SVAT models chosen for this study were developed for different purposes. The Common Land Model (CLM; Dai et al. 2001, 2003) is typically coupled with a climate model and applied at a regional or global scale. In this study, it is being used as a stand-alone model to study the ability of CLM's default land types and soil parameters to characterize the general trends in fluxes and soil states observed at a local field experiment. The Land Surface Process (LSP) model (Liou et al. 1999) is a field scale model intended to be linked with a passive microwave emission model to allow assimilation of remotely sensed microwave data to improve soil moisture estimates by SVAT models.

2. Parameterizations in the CLM and LSP models

The CLM was developed as part of a multi-institutional project to provide land surface fluxes (Dai et al. 2003) that are used as model forcings for the lower boundary of the Community Climate System Model (CCSM) (Blackmon et al. 2001) and incorporated into the Community Climate Model, version 3 (CCM3) by Zeng et al. (2002). Bonan et al. (2002) incorporated the Community Land Model, version 2 (CLM2), which is based on the original CLM, into the Community Climate System Model, version 2 (CCSM2).

Because CLM is designed to simulate land surface processes on a global scale, only simplified parameterizations of soil and canopy properties and transport mechanisms are included to minimize physical soil and vegetation parameter requirements. For each of the 18 International Geosphere–Biosphere Program (IGBP) land-cover classifications (Loveland et al. 2000), values for vegetation physical parameters are included in the model. Upon identifying the cover type, the only additional data supplied by the user are soil clay and sand percentages, soil color, latitude and longitude, and model forcings. Forcing data include downwelling solar and longwave radiation, air temperature, relative humidity, precipitation, wind speed, and atmospheric pressure.

The LSP model was developed by the University of Michigan's Microwave Geophysics group (UM-MGG) to link traditional land surface models with passive microwave emission models thus allowing data assimilation (Liou et al. 1999). Because microwave emission from a terrain is highly dependent on temperature and moisture distribution within the top 5 cm of the soil and canopy, the LSP model relies heavily upon detailed biophysically based soil and canopy properties and transport mechanisms. While assimilation is used to improve the characterization of surface moisture states, the changes in near-surface estimates will propagate down to deeper soil layers and affect land surface flux estimates in future time steps. Judge et al. (2003) describe

TABLE 1. Comparison of methods for parameterization and characterization of land surface processes for CLM and LSP.

	CLM	LSP
Parameters		
Soil texture	User defined	User defined
Porosity	Empirical calculation	User defined
Saturated hydraulic conductivity	Clapp and Hornberger	User defined
Thermal conductivity	Empirical calculation	de Vries (1963)
Wilting point	User defined	User defined
Water retention curve	Clapp and Hornberger	Rossi and Nimmo (1994)
Root depth	Empirical calculation/IGBP	User defined
Leaf area index	Empirical calculation/IGBP	User defined
Canopy height	IGBP	User defined
Roughness length	IGBP	User defined
Processes		
Soil evaporation	Diffusion	Diffusion (Philip and de Vries 1957)
Evapotranspiration	Aerodynamic (BATS and LSM based)	Aerodynamic (CLASS based)
Infiltration	Richard's equation	Richard's equation (modified)
Subsurface heat transport	Fourier's equation	Diffusion (Philip and de Vries 1957)
Runoff	Surface runoff and baseflow (TOPMODEL based)	Hortonian flow

recent modifications and further calibration to the LSP model using field observations. Within LSP, the user-provided parameters include soil texture, longitude, latitude, leaf area index (LAI), canopy height, and canopy biomass. Required weather forcings are identical to CLM except that pressure is not required.

Both CLM and LSP discretize the soil profile into layers. Each model allows soil properties to differ by layer. The soil layers' thickness increases with depth for both models. CLM has a 10-layer profile with the thickness of each layer determined by a unitless scaling factor and an exponential function that increases with depth. Given a typical vertical scaling factor of 0.025, the thickness of the uppermost layer of CLM is 1.75 cm, while the thickness of the lowest layer is 113.7 cm. The bottom depths for the eight CLM layers are 1.8, 4.5, 9.06, 16.6, 28.9, 49.3, 82.9, 138.3, 229.6, and 343.3 cm. The LSP layers' thicknesses also increase exponentially with depth to a maximum thickness of 38 cm in the bottom layer that extends from 504 to 542 cm below the ground surface. However, the LSP profile has 61 layers with 8 layers in the top 5 cm having thicknesses of 0.20, 0.54, 0.58, 0.62, 0.67, 0.72, 0.77, and 0.83 cm from the top layer to the eighth layer, respectively. Each layer's thickness may be defined as appropriate for the application. CLM has one canopy layer, while LSP has a photosynthetically active canopy layer and a thermally insulating, nonphotosynthetic thatch layer.

The parameterizations of hydrological processes, such as evapotranspiration, infiltration, and runoff vary significantly between the two models. Table 1 summarizes the differences between the parameterization schemes and the mechanisms for characterization of land surface processes for CLM and LSP. Both CLM and LSP separate precipitation into interception and throughfall based on stem and leaf area index. In CLM, surface flux estimates from multiple land-cover classifications are calculated using a tile-mosaic approach similar to Koster et al. (2000). However, because the study area contained a single vegetation type only one land cover is specified in this simulation. Both models separate bare soil evaporation from transpiration and use a diffusion approach to calculate the former and an aerodynamic approach for the latter. The aerodynamic approach refers to a scaling of the difference between the specific humidity in the atmosphere and at the canopy surface using the aerodynamic and stomatal resistances. CLM's transpiration process uses a bulk aerodynamic approach where the canopy transpiration rate has an upper bound based on the biosphere–atmosphere transfer scheme (BATS) model (Dickinson et al. 1993) and a variable stomatal resistance component from the LSM model (Bonan 1996). The surface fluxes and transpiration within the LSP are based upon the CLASS model's aerodynamic approach (Verseghy et al. 1993). While both methods use similar concepts, CLM's stomatal resistance depends on photosynthesis as related to sunlight, shade, atmospheric CO_2, atmospheric and canopy vapor pressure, temperature, foliage nitrogen, and soil water (Bonan 1996; Dai et al. 2001). LSP's stomatal resistance uses a composite value whose resistance increases as a function of incoming solar radiation, vapor pressure deficit, soil moisture suction in the root zone, and air temperature (Verseghy et al. 1993). CLM extracts transpired water from the soil layers based on the root distribution by layer as characterized by a root fraction from surface to depth z given as $f(z) = 1 - 0.5[\exp(-az) + \exp(-bz)]$ where a

and b are constants. LSP removes soil water by layer based on a weighting function that combines the root fraction, as derived from an exponential root distribution, and the soil moisture suction (Verseghy et al. 1993).

CLM and LSP use different physical approaches and numerical algorithms to linearize the nonlinear moisture and thermal transport equations. Within the soil column, CLM uses a heat diffusion approach for energy transport and Richard's equation for moisture transport. CLM determines the water movement across layer interfaces using a first-order Taylor expansion and solves the resulting equation using a tridiagonal matrix solution. The energy flux across CLM layer interfaces is solved using the Crank–Nicholson numerical scheme and a tridiagonal matrix solution (Dai et al. 2003). These methods generate soil moisture and temperature profiles at the same temporal resolution as the time step of the simulation. The LSP model simulates one-dimensional coupled moisture and energy transport in soil using the Philip and de Vries (1957) diffusion model. It uses a block-centered finite-difference approach to linearize the nonlinear coupled processes (Judge et al. 2003). The temporal resolution in the model is based on parameterized convergence criteria.

In CLM, soil physical properties are determined from the soil texture, sand and clay content, and the soil color. Estimation of soil thermal and hydraulic properties, specific heat capacity, thermal conductivity, porosity, saturated matrix potential, saturated hydraulic conductivity, and the Clapp and Hornberger (1978) B exponent ($B = 2.91 + 0.159 \times$ %clay) (Bonan 1996). The LSP model uses the Rossi and Nimmo (1994) relationship based on the Brooks and Corey (1966) formulation to estimate the retention curve and the soil texture characterized using a silt/sand/clay percent. The modification allows direct integration of the model into Mualem's (1976) hydraulic conductivity model. Infiltration processes within CLM use the Richard's equation with the inclusion of a parameterized depth of ponded water used for minimal detention storage between time steps. In the LSP model, the infiltration rate is estimated using a quasi-analytic solution to Richard's equation for vertical infiltration in a homogeneous soil with a constant initial moisture profile (Green and Ampt 1911; Philip 1957, 1987, 1990).

LSP generates runoff by saturation excess with the depth of runoff corresponding to the water not infiltrated at the end of each time step. CLM's surface runoff is based upon the watershed scale model TOPMODEL (Beven et al. 1995) as adapted for land surface modeling (Stieglitz et al. 1997). Details on CLM's runoff scheme are presented by Niu et al. (2005). To summarize, a CLM grid cell consists of saturated and unsaturated areas determined from a three-parameter gamma distribution of the topographic index. Separate surface and subsurface runoff calculations are performed over the saturated and unsaturated areas of the watershed. All precipitation runs off of the saturated area while the soil moisture in the top three layers controls surface runoff in unsaturated areas. For the saturated area, subsurface runoff is determined using a TOPMODEL approach based on the estimated water table depth (Dai et al. 2001). Saturated hydraulic conductivity decreases exponentially with depth. The unsaturated area estimates vertical drainage based on the saturated hydraulic conductivity of the lower layers using the BATS approach (Dickinson et al. 1993).

The TOPMODEL approach to estimating surface runoff and baseflow generation mechanisms is reasonable for CLM. CLM is intended to be used on a regional or global scale. TOPMODEL can provide effective runoff characterization at this scale. Because wetlands have low topographic relief, little or no channelization, and strong confining layers, modeling drainage using the TOPMODEL approach will likely overpredict vertical drainage. To examine the effect of the TOPMODEL runoff characterization, in this study the soil column was simulated using two scenarios. The first applies the CLM subsurface runoff generation mechanism without modification. The second eliminates subsurface runoff and uses a no-flux boundary condition at the lowest soil layer.

3. Study area and experimental observations

The study was conducted in a wet prairie subcommunity in the Paynes Prairie Preserve, a large highland marsh ecosystem (29°34′14″N, 82°16′46″W). Paynes Prairie State Preserve is a 5600-ha regional basin in north-central Florida that contains marsh wetland communities and pasture. The study site is a relatively flat, treeless plain with moderately dense ground cover. Typically, this site is inundated for 50 to 100 days each year. The site's soils include Emeralda fine sandy loam, Wauberg sand, and Ledwith Muck. The soils consist of sands with an organic surface layer that are underlain by clay. Field observations showed that the majority of the root zone was contained in the upper 10-cm soil layer with approximately 95% of the root zone contained in the upper 25-cm soil layer. The mean canopy height during the study period is approximately 1.0 m.

A tower-based eddy flux and meteorological station were located in the prairie wetland. Jacobs et al. (2002a) provide a complete description of the instrumentation, study area, and data development. Near-

surface volumetric soil water content was recorded by CS615 moisture probes at three depths: 7.6, 12.7, and 17.8 cm. The probe's measurement error is ±2.5% volumetric water content. The soil temperature was measured with a CS107 temperature probe at the same depths with an additional temperature measurement at 2.5 cm. Measurement error associated with the temperature probe is ±0.5 K. Thirty-minute average values of net radiation, latent heat flux, sensible heat flux, and ground heat flux were recorded.

The study period is during a steady dry-down condition from 4 to 17 May 2001 during which the depth to the water table increased from 62 to 86 cm. The period is characteristic of the transition from first stage (potential) to second stage (limited) soil water conditions (Brutsaert and Chen 1995) as defined by soil moisture (Jacobs et al. 2002a). There was no precipitation during the study period. The study period occurs within a 40-day dry down from saturated conditions from 17 April until 27 May. The period leading up to the study period, 17 April to 3 May had no rainfall events exceeding 0.3 mm. Prior to the dry down, the water table was above the surface from mid-March to mid-April 2001.

4. Simulation design

a. Forcings

Meteorological observations during the experiment described in section 3 were used to force the CLM and LSP models. Required forcings are comparable to the measurements except for atmospheric pressure. Estimates of incoming short- and longwave radiation were derived from measured net radiation. Daytime values of the longwave radiation balance were estimated using Diak et al.'s (2000) remotely sensed radiation estimation scheme based on Geostationary Operational Environmental Satellite (GOES) data (Jacobs et al. 2002b). The diurnal surface albedo was determined for a cloud-free day using measured incoming shortwave radiation, measured net radiation, and GOES estimated net longwave.

b. Initialization

The CLM and LSP initialization schemes require the initial soil temperature profile and the initial soil moisture content profile. The soil temperature profile is initialized using measured values for the top 23 cm. For the lower profile, the initial temperature is set equal to the temperature measured at 23 cm. The soil moisture profile is initialized using measurements in the top 17 cm of the profile. The profile is saturated below 62 cm. Because no measurements were available below 17 cm and soil water suction and hydraulic conductivity are relatively constant between the 0.20 $m^3\ m^{-3}$ value at 17 cm and the saturated 0.30 $m^3\ m^{-3}$ value at the water table, the initial soil moisture is assumed to increase linearly with depth between 17 cm and the water table.

c. Parameterization

Soil texture was determined based on the soil composition of Wauberg Sand from the Soil Characterization Laboratory soil composition profile (University of Florida-Institute of Food and Agricultural Sciences 1985). The soil texture is classified as predominantly sand (~95%) from the soil surface to 0.61 m, clay sand to 2.1 m, and sandy clay below 2.1 m. Based on field observations, the top 2 cm had a high organic content. The soil texture values for the Wauberg Sand layers were interpolated vertically to obtain the 10 CLM layers. CLM's soil characteristics gradually transition from 95.2% sand and 3.3% clay in the top three layers to 41.6% sand and 43.8% clay in the bottom layer. LSP's top two layers were characterized as 50% sand and 3.3% clay. The remaining LSP layers were based on UF-IFAS soil texture characteristics. CLM's Clapp and Hornberger B parameters range from 3.4 for the top layer to 9.9 for the bottom layer. CLM's parameterization scheme results in an exponential decrease of saturated hydraulic conductivity with depth while LSP's saturated hydraulic conductivity is approximately constant below 1 m.

Table 2 summarizes the vegetation parameters used in the CLM and LSP models. LSP's vegetation parameters are user defined based on observations, while reflectance and transmittance values are calculated for each time step based on canopy characteristics and solar angle. CLM uses the IGBP land-cover types with default plant physiology (leaf optical properties, stomatal physiology, leaf dimension) and vegetation structure (height, roughness length, displacement height, root profile, monthly leaf, and stem area) characteristics for land cover. Because marsh is not one of the 18 IGBP land-cover classifications, the broader parameters for a "permanent wetland" were used. However, the vegetation types found within a permanent wetland can greatly differ from the vegetation types found in a prairie wetland marsh community. Prairie wetland vegetation changes annually in response to recent hydroperiods. A relatively dry multiyear period preceded the study period and resulted in uplands plants consistent with pastures (Jacobs et al. 2002a). Because the near-infrared reflectance and transmittance parameters for a permanent wetland absorb more shortwave radiation than that of a grassland, the values of near-infrared

TABLE 2. Vegetation parameters used by CLM and LSP.

	CLM[a]	LSP
Maximum leaf area index (-)	6	3.5[b]
Minimum leaf area index (-)	0.5	2.0[b]
Stem area index (-)	2	N/A
Aerodynamic roughness length (m)	0.25	0.05[b]
Displacement height (m)	1	0.35[b]
Leaf dimension (m)	0.04	N/A
Visible leaf reflectance	0.11	Calc[c]
Near-infrared leaf reflectance	0.58	Calc[c]
Visible stem reflectance	0.36	Calc[c]
Near-infrared stem reflectance	0.58	Calc[c]
Visible leaf transmittance	0.07	Calc[c]
Near-infrared leaf transmittance	0.25	Calc[c]
Visible stem transmittance	0.22	Calc[c]
Near-infrared stem transmittance	0.38	Calc[3]
Root parameters	$a = 2, b = 6$[d]	$Z_r = 1$[e]
Canopy top height (m)	0.5	0.5
Canopy bottom height (m)	0.01	0

[a] All CLM parameters were taken from the IGBP land-cover classification.
[b] LSP canopy data were input based on measured data.
[c] LSP reflectance and transmittance values are calculated for each time step based on solar angle.
[d] a (m^{-1}) and b (m^{-1}).
[e] $R(z) = [\exp(-3z) - \exp(-3z_r)]/[1 - \exp(-3z_r)]$, where z and z_r (m) (Verseghy et al. 1993).

reflectance and transmittance for "grasslands" were used.

5. Results

The simulation results are evaluated by comparing the modeled soil moisture, soil temperature, and surface heat fluxes with measured field data. To avoid overemphasizing extreme values, the mean absolute error (MAE), which is less sensitive to large differences (Willmott 1982), is reported in addition to the root-mean-squared error (RMSE).

a. CLM subsurface runoff intercomparison

CLM was used to model the study site using the two subsurface runoff generation scenarios. The first scenario utilizes the default CLM subsurface runoff mechanism that exports water from the soil column based on a function of the soil parameters and the estimated water table depth. The second scenario eliminates the subsurface runoff generation mechanism within CLM and removes no soil water through baseflow. Figure 1 illustrates that the first scenario results in a physically unrealistic drying out of the soil column, particularly at the lower depths, as compared to both the second scenario and measured results. As the soil dried, low and high biases were also observed for the

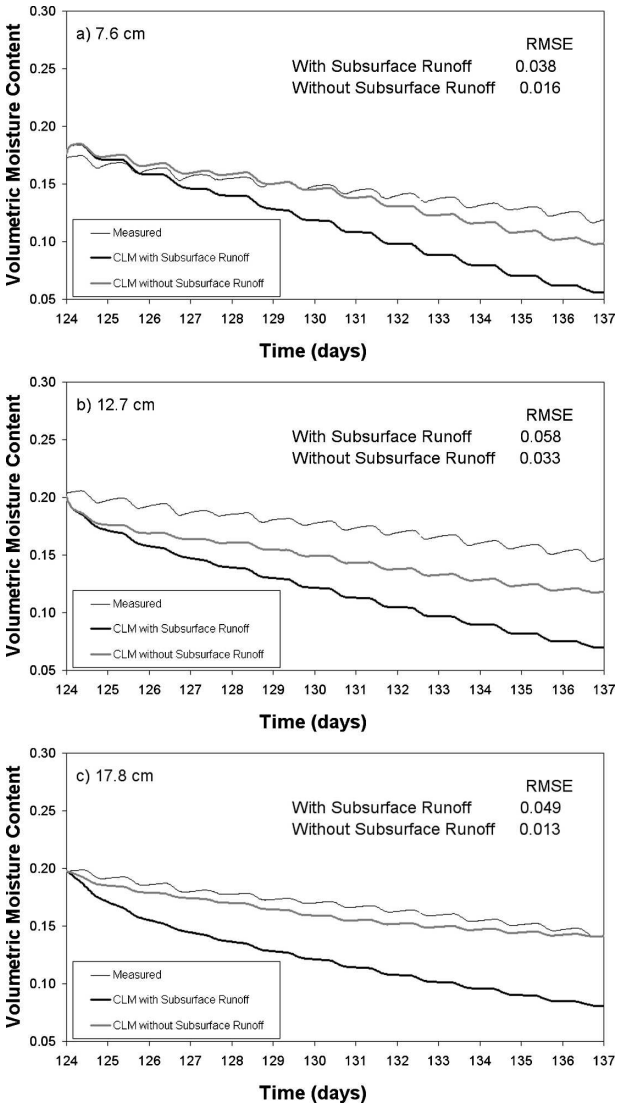

FIG. 1. Comparison of measured volumetric soil moisture ($m^3\ m^{-3}$) with CLM using both TOPMODEL subsurface runoff generation processes and no subsurface runoff generation at (a) 7.6, (b) 12.7, and (c) 17.8 cm. RMSE units are $m^3\ m^{-3}$.

modeled latent and sensible heat fluxes, respectively. Given that the baseline runoff approach of CLM results in an unrealistic drying of the soil column, the following sections use CLM without subsurface baseflow.

b. CLM and LSP intercomparison

1) SOIL MOISTURE

The observed measurements of soil moisture were compared to the simulated moisture for the CLM and LSP soil layer that contained the measurement point. Figure 2 shows the evolution of modeled and measured soil moisture and summary statistics during the study period. Measured values at 7.6 cm showed a 5–6 $m^3\ m^{-3}$

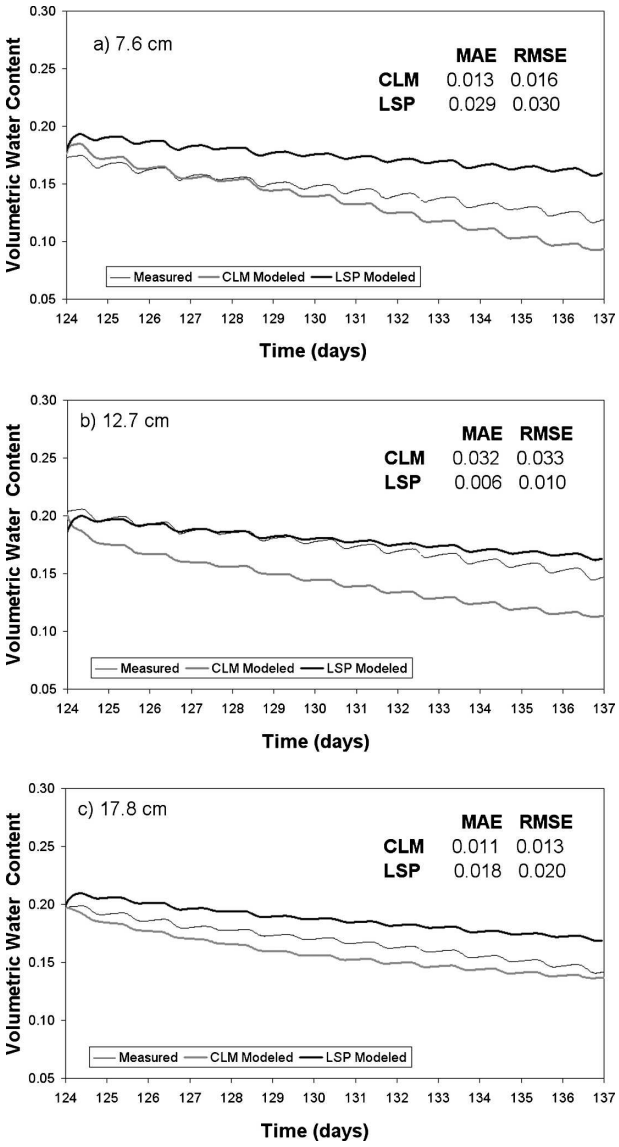

FIG. 2. Comparison of measured volumetric soil moisture ($m^3\ m^{-3}$) with CLM and LSP modeled at (a) 7.6, (b) 12.7, and (c) 17.8 cm. RMSE and MAE units are $m^3\ m^{-3}$.

decrease in soil moisture over 14 days. CLM's top layer at 7.6 cm has a higher modeled water content than observed during the first two days of the experiment. However, the relatively high dry-down rate resulted in the simulated layer having lower moisture than the observed beginning on day 128. The bias increased over the study duration. The LSP model simulated a dry-down rate at the 7.6-cm layer of 3 $m^3\ m^{-3}$ over the 14-day period, which matches the observed rate. The initial offset in the modeled soil moisture results in a bias of about 3 $m^3\ m^{-3}$ for the entire experimental period.

In general, both models captured the magnitude and depth of soil water extraction due to evapotranspiration as well as the daytime fluctuations in moisture. LSP simulated the complete phase and amplitude of the measured soil moisture more realistically throughout the experiment period. Differences between the observed and the LSP modeled moisture were largely due to the soil water profile rapidly equilibrating to a profile with a slight wet bias. This profile reflects LSP's soil physical properties and suggests that the model properties differ somewhat from those found at the site.

The LSP model simulated realistic soil moisture at 12.7 cm with a low MAE of 0.006 $m^3\ m^{-3}$, while the CLM soil moisture values showed increasing negative bias over the duration resulting in a MAE of 0.03 $m^3\ m^{-3}$. Both CLM and LSP provide reasonable moisture content estimates at the deepest measurement depth (17.8 cm). CLM's moisture contents are slightly drier (0.01 $m^3\ m^{-3}$) than measured, while LSP's modeled water contents are slightly wetter (0.02 $m^3\ m^{-3}$).

While, CLM's daytime dry down appears to function appropriately, CLM was unable to replicate the movement of water upward from the wetter, lower layers. For example, in the top layer the soil moisture measurements typically declined by 0.7 $m^3\ m^{-3}$ during daytime, but increased by 0.4 $m^3\ m^{-3}$ during nighttime for a net decrease of approximately 0.3 $m^3\ m^{-3}$. Daytime root water extraction from the surface layers results in an observed soil water profile that increases with depth. The large gradient of soil matric potentials drives soil water upward in the soil profile during the evening as measured and modeled by LSP. However, CLM's soil moisture values remain constant at night. That LSP and CLM results differ is likely due to variations in soil water retention curves, unsaturated hydraulic conductivity, and possibly LSP's much shorter time step.

The volumetric soil moisture errors identified in this study are consistent with other studies' results. In PILPS phase 2(b), Shao and Henderson-Sellers (1996) recognized ±3% volumetric water content error margins as reasonable, while Mohr et al. (2000) found error margins in near-surface soil simulations of ±5% volumetric soil moisture. To some degree, these error ranges reflect typical instrumentation measurement errors associated with a CS615 moisture probe.

2) SOIL TEMPERATURE

The modeled and observed soil temperature profile comparison follows the soil moisture comparison with an additional temperature measurement at 2.5-cm depth (Fig. 3). Overall, both models show good agreement with the observed phase and amplitude of the diurnal fluctuations and capture the warming trend over the study period. A strong diurnal temperature

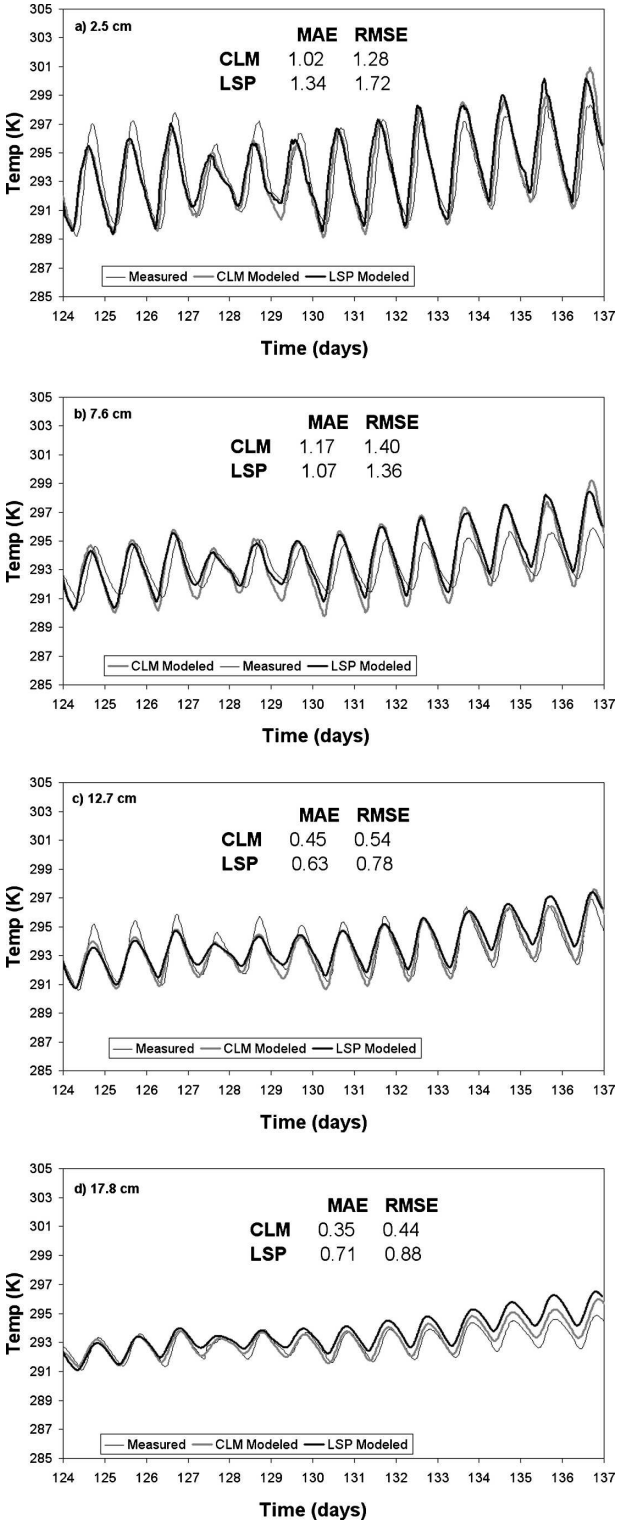

FIG. 3. Comparison of measured subsurface soil temperature and CLM and LSP modeled soil temperature at (a) 2.5, (b) 7.6, (c) 12.7, and (d) 17.8 cm. RMSE and MAE units are K.

signature was observed and ranged from 6 K at 2.5 cm to 2 K at 17.8 cm. CLM's simulated diurnal temperature range typically exceeded LSP's range by approximately 1 K. This could be the result of the different parameterizations used by the two models to simulate heat transport in the soil. Despite higher moisture contents, LSP's soil temperatures generally show higher fluctuations in temperature than the measurements. The smallest temperature errors occur in the 12.7-cm layer where LSP soil moisture most closely matches measurements. Soil moisture errors would cause invalid soil heat capacity estimates and incorrect thermal transport of energy in the soil. At 7.6 cm, simulations from both models lead measured diurnal fluctuations by 2 to 3 h throughout the study period. Lower layers do not have this discrepancy.

Measured values at 2.5 cm increased by 1.5 to 2 K during the experiment period, reflecting observed dry down and warming conditions. For the top layer, modeled temperatures underestimated peaks during the initial period, but overestimated daily maxima by up to 3 K at the experiment's end. At 7.6 cm, simulated maxima for both models are within 1 K of measured maximum early in the experiment, but differences reach up to 3.0 K by the end of the experiment. At 12.7 cm, the modeled diurnal cycles early in the simulation period are slightly underestimated. Agreement improves during the experimental period with the final diurnal cycle exhibiting good agreement with the measurements. The deepest measurements at 17.8 cm compare well with both simulated time series for the first 10 days while the final three days showed a small warm bias.

For both models, modeled errors decrease with depth because diurnal fluctuations are damped by the increasing soil thickness. The largest errors, occurring in the top two layers for both models, fell within 3 times the instrument error of ± 0.5 K. These results compare reasonably well with similar modeling studies. Both Chen et al. (1997) and Mohr et al. (2000) found errors within ± 2 K for subsurface temperatures. Offline simulations of PILPS phase 1 found ranges between models of 1.4 K for tropical forest and 2.2 K for grassland in a multiyear study. Similar studies of the LSP model have resulted in average differences of 0.1 K between modeled and observed temperatures in the top 10 cm of soil for winter wheat stubble (Judge et al. 1999) and differences of 1.8 and 1.0 K for bare soil and brome grass, respectively.

3) SURFACE HEAT FLUXES

Figure 4 compares modeled energy fluxes with field observations. The MAE and RMSE values in Fig. 4

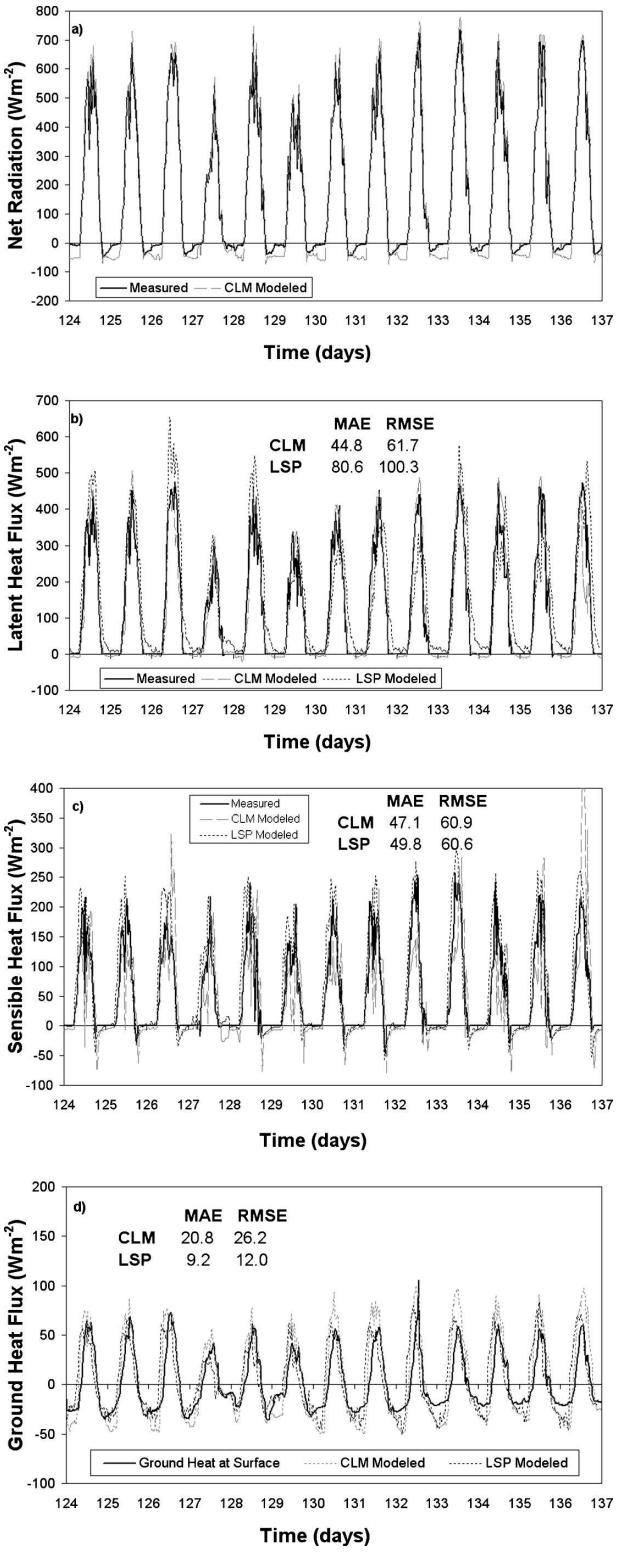

FIG. 4. Comparison of modeled and measured surface fluxes for (a) CLM net radiation, (b) CLM and LSP latent heat flux, (c) CLM and LSP sensible heat flux, and (d) CLM and LSP ground heat flux at the surface. MAE and RMSE values are in W m^{-2}.

were calculated using only daytime values (0600 until 1830) due to missing nighttime measurements. Both models captured the diurnal variation in all energy fluxes. Figure 4a shows that net radiation modeled by the CLM and measured net radiation agree well. As mentioned before, while the IGBP land-cover classification was wetland, the grassland reflectance and transmittance parameters provided a much better fit than the wetland parameters. Because both downwelling longwave and shortwave radiation force CLM, this agreement demonstrates the accuracy of simulated reflected radiation or albedo and upwelling longwave radiation. These results also ensure that the models are forced using the available energy as observed. Because the LSP model's albedo function is generated using a curve fitting the observations, a net radiation comparison is not valid.

CLM's latent heat flux estimates are more realistic than LSP estimates, with errors typically less than 20% of the average measured latent heat flux (232.1 W m^{-2}). On average, CLM latent heat fluxes are within 10 W m^{-2} (4.1%) of observed values. In contrast, LSP results have a large discrepancy between simulated and measured fluxes for latent heat fluxes. For a given day, LSP either underestimates or overestimates midday evaporative fluxes. The result is that the MAE of the LSP simulation is 37% of the average measured latent heat flux and, on average, measured fluxes are overestimated by 27 W m^{-2} (10.5%). The LSP model overestimates on day 126 by ~200 W m^{-2} resulted in a high RMSE of 100 W m^{-2} for the study period. Eddy covariance systems, used to measure latent and sensible heat fluxes, typically have average errors of about 30 W m^{-2} due to issues with energy closure (Twine et al. 2000).

Both CLM and the LSP model have comparable agreement for sensible heat fluxes with MAE errors of approximately 50% of the average measured sensible heat flux (98.7 W m^{-2}). The CLM model overestimates daily maximas significantly during days 126 and 136. This resulted in a high RMSE of 60.9 W m^{-2}. The sensible heat flux estimates by the LSP model are more consistently realistic than the CLM estimates.

The heat flux measured at the depth of 10 cm was added to the soil heat storage in the 0–10-cm layer to calculate ground heat flux. LSP and CLM's ground heat fluxes are compared to calculated ground heat fluxes (Fig. 4). The MAE for the CLM daytime simulated ground heat fluxes is nearly equal to the average magnitude of the measured ground heat fluxes (22.6 W m^{-2}). The LSP daytime simulated ground heat fluxes are quite reasonable throughout the experiment. Note that in both the models, ground heat flux is a residual

term and large errors in latent heat fluxes in the LSP model resulted in very small errors in the ground heat flux to maintain the energy balance. Similarly, the low errors in latent and sensible heat flux simulations from the CLM model resulted in a relatively high error in the ground heat flux measurements.

Surface flux simulations often provide the largest discrepancies from measurements. Chen et al. (1997) found reasonable agreement with ranges across modeling schemes of 30 and 25 W m^{-2} for sensible and latent heat flux, respectively. Chang et al. (1999) also found good agreement using the coupled atmosphere–plant–soil model, with a monthly discrepancy of 7.1 W m^{-2} in latent heat flux and 7.7 W m^{-2} for sensible heat flux. However, the same study found discrepancies in diurnal amplitude of ground heat flux around 20 W m^{-2} with a phase difference of 2.5 h. Both Chen et al. (1997) and Chang et al. (1999) calculated error margins based on the full diurnal cycle. A trend evident in several SVAT model validation studies (Acs and Hantel 1998; Chang et al. 1999; Gonzalez-Sosa et al. 2001) shows that latent heat fluxes are more accurately simulated than sensible heat fluxes and ground heat fluxes. This trend suggests that the model physics representing the processes of latent heat flux are more comprehensive than the model physics describing sensible or ground heat fluxes. The results of the CLM simulation provide another example of this tendency. In contrast, the LSP model has more sophisticated sensible and ground heat flux processes than the latent heat flux processes.

6. Discussion

Based on the preceding analysis of the figures and the error statistics, the model results seem to be quite reasonable. Both LSP and CLM provide realistic simulations of fluxes and soil temperature and moisture. The soil's warming trend and its diurnal temperature fluctuations are well represented. These findings suggest potential application to biogeochemical and plant dynamic studies whose conditions are strongly influenced by soil temperature. Some issues were identified. Both models gradually, but consistently, diverge from measured temperature and water states. Their top diurnal temperature fluctuations lead measured values by 2 to 3 h. LSP's latent heat fluxes had large midday errors.

The findings also raise some serious concerns for the application of SVATs to wetlands, particularly at a field scale. An immediate challenge for CLM is that its drainage approach is not appropriate for this marsh wetland because it will rapidly dewater the site. Further investigations across other wetland sites are required to determine if this is a systematic issue. If so, other drainage parameterizations that do not depend on TOPMODEL parameter may be required.

While the water table constrains the root zone in wetlands and other high water table environments, CLM's exponential root zone function is independent of water table. As a result, the default CLM wetland root zone is much deeper than observed. Furthermore, CLM did not move water in the vadose zone from lower to upper layers during the nighttime as observed in the measurements. The cause and importance of this movement is not known at scales exceeding the field scale and requires further investigation. Interestingly, the combined effect of an excessively deep root zone and limited upward water movement may have resulted in latent heat fluxes being reasonable as the errors negated each other. Although the top layer was too dry, the canopy was not stressed because adequate water for transpiration was available from the lower depths.

A significant success was that LSP, developed for prairie grasslands, was able to characterize the wetland dynamics with no changes to the model's physical processes. The inconsistent errors in evapotranspiration suggest that Verseghy et al.'s (1993) resistance functions need to be adjusted for wetland conditions. If limited data exist to modify these functions, CLM's more successful approach should be considered. Finally, LSP's rapid vertical movement of soil water is of considerable interest. Problematically, the initial soil water profile was rapidly reestablished at values that differed from initial conditions. However, LSP provided an excellent characterization of the upward soil water movement at night. An understanding of the overall impact of soil water dynamics requires studies to be conducted over longer periods.

7. Conclusions

The purpose of this research was to compare two SVAT models' applicability in a marsh wetland in the southeastern United States for a 13-day dry-down period. While all SVAT models rely on similar mathematical approximations of biophysical reality, differences among models result from their original function as reflected in the choice of model physics, number of soil layers, soil and vegetation parameterization, and numerical solution methods. Here, the results indicate that both models were able to reasonably simulate the water and energy dynamics. CLM's climate modeling history showed in its flux modeling success, but weaknesses were revealed in characterizing soil water. For this study, realistic soil moisture simulations were only possible after CLM's baseline TOPMODEL baseflow

generation mechanism was removed. In contrast, LSP's origins in characterizing soil profile conditions for microwave brightness modeling resulted in better results for the profiles than the fluxes.

Specific challenges for using these SVATs to model marsh communities were the high water table and vegetation characteristics. Prior to applying SVAT models to low relief topography or high water table regions, the SVAT's deep drainage and baseflow generation mechanism as well as its ability to transport water upward in the soil column should be examined. In addition, wetlands include a wide variety of plants that may not be readily characterized by broad vegetation parameters. Issues identified by this study were that CLM's wetland IGBP vegetation class requires some pasture parameters, CLM's rooting depths greatly exceed observed depths, and LSP's canopy resistance scaling functions may result in both the over- and underestimation of latent heat fluxes.

Overall, this relatively brief experiment demonstrates the potential for the application of SVAT models in marsh communities during a dry down. However, additional studies are needed that include the seasonal and interannual wetland hydroperiods having a full range of conditions, including flood, drought, and burning, to identify issues related to long-term simulation.

Acknowledgments. Support for this work was provided by the NASA NIP Grant NAG5-10567. The NASA Summer Institute sponsored B. Whitfield's CLM work under the guidance of P. Houser, NASA Goddard Space Flight Center. We thank A. Lopera, S. Mergelsberg, and D. Myers for their role in collecting the field dataset. L. C. Friess is acknowledged for her editorial contribution. Three anonymous reviewers are thanked for their helpful comments and suggestions.

REFERENCES

Acs, F., and M. Hantel, 1998: The land-surface flux model PROGSURF. *Global Planet. Change,* **19,** 19–34.

Beven, K. J., R. Lamb, P. Quinn, R. Romanowicz, and J. Freer, 1995: Topmodel. *Computer Models of Watershed Hydrology,* V. P. Singh, Ed., Water Resource Publications, 627–668.

Blackmon, M., and Coauthors, 2001: The Community Climate System Model. *Bull. Amer. Meteor. Soc.,* **82,** 2357–2376.

Bonan, G. B., 1996: A land surface model (LSM version 1.0) for ecological, hydrological, and atmospheric studies: Technical description and user's guide. NCAR Tech. Note NCAR/TN-417+STR, 150 pp.

——, K. W. Oleson, M. Vertenstein, S. Levis, X. B. Zeng, Y. J. Dai, R. E. Dickinson, and Z. L. Yang, 2002: The land surface climatology of the community land model coupled to the NCAR community climate model. *J. Climate,* **15,** 3123–3149.

Brooks, R. H., and A. T. Corey, 1966: Properties of porous media affecting fluid flow. *J. Irrig. Drain. Div. Amer. Soc. Civ. Eng.,* **92,** 61–87.

Brutsaert, W., and D. Chen, 1995: Desorption and the two stages of drying of natural tallgrass. *Water Resour. Res.,* **31,** 1305–1313.

Chang, S., D. Hahn, C. H. Yang, and D. Norquist, 1999: Validation study of the CAPS model land surface scheme using the 1987 Cabauw/PILPS dataset. *J. Appl. Meteor.,* **38,** 405–422.

Chen, T. H., and Coauthors, 1997: Cabauw experimental results from the project for intercomparison of land-surface parameterization schemes. *J. Climate,* **10,** 1194–1215.

Clapp, R. B., and G. M. Hornberger, 1978: Empirical equations for some soil hydraulic-properties. *Water Resour. Res.,* **14,** 601–604.

Comer, N. T., P. M. Lafleur, N. T. Roulet, M. G. Letts, M. Skarupa, and D. Verseghy, 2000: A test of the Canadian Land Surface Scheme (CLASS) for a variety of wetland types. *Atmos.–Ocean,* **38,** 161–179.

Dai, Y., X. Zeng, and R. Dickinson, 2001: Common Land Model (CLM): Technical documentation and user's guide. 69 pp. [Available online at climate.eas.gatech.edu/dai/clmdoc.pdf.]

——, and Coauthors, 2003: The Common Land Model. *Bull. Amer. Meteor. Soc.,* **84,** 1013–1023.

de Vries, D. A., 1963: Thermal properties of soils. *Physics of Plant Environment,* Interscience Publishers, 210–235.

Diak, G. R., W. L. Bland, J. R. Mecikalski, and M. C. Anderson, 2000: Satellite-based estimates of longwave radiation for agricultural applications. *Agric. For. Meteor.,* **103,** 349–355.

Dickinson, R. E., A. Henderson-Sellers, and P. J. Kennedy, 1993: Biosphere–Atmosphere Transfer Scheme (BATS) version 1e coupled to the NCAR Community Climate Model. NCAR Tech. Note NCAR/TN-387+STR, 72 pp.

Dirmeyer, P. A., A. J. Dolman, and N. Sato, 1999: The pilot phase of the Global Soil Wetness Project. *Bull. Amer. Meteor. Soc.,* **80,** 851–878.

Gonzalez-Sosa, E., I. Braud, J. L. Thony, M. Vauclin, and J. C. Calvet, 2001: Heat and water exchanges of fallow land covered with a plant-residue mulch layer: A modeling study using the three year MUREX data set. *J. Hydrol.,* **244,** 119–136.

Green, W., and G. Ampt, 1911: Studies on soil physics. *J. Agric. Sci.,* **4,** 1–24.

Hall, J. V., W. E. Frayer, and B. O. Wilen, 1994: Status of Alaska Wetlands. U.S. Fish and Wildlife Service, Alaska Region, Anchorage, AK, 32 pp.

Henderson-Sellers, A., A. J. Pitman, P. K. Love, P. Irannejad, and T. H. Chen, 1995: The Project for Intercomparison of Land-Surface Parameterization Schemes (PILPS): Phase-2 and Phase-3. *Bull. Amer. Meteor. Soc.,* **76,** 489–503.

Jacobs, J. M., S. L. Mergelsberg, A. F. Lopera, and D. A. Myers, 2002a: Evapotranspiration from a wet prairie wetland under drought conditions: Paynes Prairie Preserve, Florida, USA. *Wetlands,* **22,** 374–385.

——, D. A. Myers, M. C. Anderson, and G. R. Diak, 2002b: GOES surface insolation to estimate wetlands evapotranspiration. *J. Hydrol.,* **266,** 53–65.

Judge, J., A. W. England, W. L. Crosson, C. A. Laymon, B. K. Hornbuckle, D. L. Boprie, E. J. Kim, and Y.-A. Liou, 1999: A growing season Land Surface Process/Radiobrightness model for wheat-stubble in the southern Great Plains. *IEEE Trans. Geosci. Remote Sens.,* **37,** 2152–2158.

——, L. M. Abriola, and A. W. England, 2003: Numerical validation of the land surface process component of the LSP/R model. *Adv. Water Resour.,* **26,** 733–746.

Kim, E. J., 1999: Remote sensing of land surface conditions in arctic tundra regions for climatological applications using microwave radiometry. Ph.D. thesis, University of Michigan, 172 pp.

Koster, R. D., M. J. Suarez, A. Ducharne, M. Stieglitz, and P. Kumar, 2000: A catchment-based approach to modeling land surface processes in a general circulation model. 1. Model structure. *J. Geophys. Res.,* **105,** 24 809–24 822.

Lafleur, P. M., 1990: Evapotranspiration from sedge-dominated wetland surfaces. *Aquat. Bot.,* **37,** 341–353.

Liang, X., and Coauthors, 1998: The Project for Intercomparison of Land-surface Parameterization Schemes (PILPS) phase 2(c) Red–Arkansas River basin experiment: 2. Spatial and temporal analysis of energy fluxes. *Global Planet. Change,* **19,** 137–159.

Liou, Y. A., J. F. Galantowicz, and A. W. England, 1999: A land surface process radiobrightness model with coupled heat and moisture transport for prairie grassland. *IEEE Trans. Geosci. Remote Sens.,* **37,** 1848–1859.

Loveland, T. R., B. C. Reed, J. F. Brown, D. O. Ohlen, Z. Zhu, L. Yang, and J. W. Merchant, 2000: Development of a global land cover characteristics database and IGBP DISCover from 1 km AVHRR data. *Int. J. Remote Sens.,* **21,** 1303–1330.

Mitsch, W. J., and J. G. Gosselink, 2000: *Wetlands.* 3d ed. John Wiley & Sons, 920 pp.

Mohr, K. I., J. S. Famiglietti, A. Boone, and P. J. Starks, 2000: Modeling soil moisture and surface flux variability with an untuned land surface scheme: A case study from the southern Great Plains 1997 Hydrology Experiment. *J. Hydrometeor.,* **1,** 154–169.

Mualem, Y., 1976: A new model for predicting the hydraulic conductivity of unsaturated porous media. *Water Resour. Res.,* **12,** 513–522.

Nijssen, B., I. Haddeland, and D. P. Lettenmaier, 1997: Point evaluation of a surface hydrology model for BOREAS. *J. Geophys. Res.,* **102,** 29 367–29 378.

Niu, G. Y., Z. L. Yang, R. E. Dickinson, and L. E. Gulden, 2005: A simple TOPMODEL-based runoff parameterization (SIMTOP) for use in global climate models. *J. Geophys. Res.,* **110,** D21106, doi:10.1029/2005JD006111.

Philip, J. R., 1957: Theory of infiltration. 1. The infiltration equation and its solution. *Soil Sci.,* **83,** 345–357.

——, 1987: The infiltration joining problem. *Water Resour. Res.,* **23,** 2239–2245.

——, 1990: Inverse solution for one-dimensional infiltration, and the ratio A/K_1. *Water Resour. Res.,* **26,** 2023–2027.

——, and D. de Vries, 1957: Moisture movement in porous materials under temperature gradients. *Trans. Amer. Geophys. Union,* **38,** 222–232.

Pitman, A. J., and Coauthors, 1999: Key results and implications from phase 1(c) of the Project for Intercomparison of Land-Surface Parameterization Schemes. *Climate Dyn.,* **15,** 673–684.

Rossi, C., and J. R. Nimmo, 1994: Modeling of soil-water retention from saturation to oven dryness. *Water Resour. Res.,* **30,** 701–708.

Shao, Y. P., and A. Henderson-Sellers, 1996: Validation of soil moisture simulation in landsurface parameterization schemes with HAPEX data. *Global Planet. Change,* **13,** 11–46.

Slater, A. G., and Coauthors, 2001: The representation of snow in land surface schemes: Results from PILPS 2(d). *J. Hydrometeor.,* **2,** 7–25.

Souch, C., C. P. Wolfe, and C. S. B. Grimmond, 1998: Evapotranspiration rates from wetlands with different disturbance histories: Indiana Dunes National Lakeshore. *Wetlands,* **18,** 216–229.

Stieglitz, M., D. Rind, J. Famiglietti, and C. Rosenzweig, 1997: An efficient approach to modeling the topographic control of surface hydrology for regional and global climate modeling. *J. Climate,* **10,** 118–137.

Twine, T. E., and Coauthors, 2000: Correcting eddy-covariance flux underestimates over a grassland. *Agric. For. Meteor.,* **103,** 279–300.

University of Florida-Institute of Food Agricultural Sciences, 1985: Characterization data for selected soils. Soil Science Research Rep. 85-1.

van der Keur, P., S. Hansen, K. Schelde, and A. Thomsen, 2001: Modification of DAISY SVAT model for potential use of remotely sensed data. *Agric. For. Meteor.,* **106,** 215–231.

Verseghy, D. L., N. A. McFarlane, and M. Lazare, 1993: Class—A Canadian Land-Surface Scheme for Gcms. 2. Vegetation model and coupled runs. *Int. J. Climatol.,* **13,** 347–370.

Willmott, C. J., 1982: Some comments on the evaluation of model performance. *Bull. Amer. Meteor. Soc.,* **63,** 1309–1313.

Zeng, X. B., M. Shaikh, Y. J. Dai, R. E. Dickinson, and R. Myneni, 2002: Coupling of the Common Land Model to the NCAR Community Climate Model. *J. Climate,* **15,** 1832–1854.

Zhang, Y., C. Li, C. C. Trettin, H. Li, and G. Sun, 2002: An integrated model of soil, hydrology, and vegetation for carbon dynamics in wetland ecosystems. *Global Biogeochem. Cycles,* **16,** 1061, doi:10.1029/2001GB001838.